

Flowing Field Analysis and Experiment of the Electroforming of Micro-Hole Array Mold Insert

Ming-Nan Fu^{1*}, Ching-Chung LI², and Yih-Min Yeh³

¹ Department of Industrial Engineering and Management, Asian-Pacific Institute of Creativity.

² Department of Information Management, Ching Yun University.

³ Graduate School of Opto-Mechatronics and Materials, Wu Feng University.

ABSTRACT

This paper study uses computational fluid simulation to build models for the electroforming flow field of a micro-hole array mold insert, and discusses flow field effects and stress distribution in detail. Simulation results demonstrate that similar aperture sizes with a low aspect ratio improved the plating solution interchange rate. The plating solution interchange rate with large aperture and fast entry flow speed is better. The enhanced rotational speed of the cathode can increase the upward flush speed for a small hole. Via centrifugal force, it specify can increase the carrying speed of an old plating solution for a small hole and low entry flow speed. In the characteristics of a multi-hole array, an overly high rotation rate for the cathode plate in a plating tank does not substantially assist. Using a low rotation rate to carry out during process with different sizes and specifications, reduces cost, and increases production quality. This can be regarded as an important reference for multi-usage of micro-hole array mold insert design and production.

Keywords: array mold insert, aspect ratio, micro-electroforming, flow field distribution

不同尺寸微孔洞陣列模仁電鑄流場分析與實作

傅明南^{1*} 李慶忠² 葉翳民³

¹ 亞太創意技術學院工業工程與管理系

² 清雲科技大學資訊管理系

³ 吳鳳科技大學光機電暨材料研究所

摘 要

本文針對微孔洞陣列模仁電鑄流場，以計算流體的方法配合電腦軟體建立模型，並針對其中的流場效應及應力分布作深入探討，透過電腦數值模擬可以發現，低深寬比對鍍液交換效果明顯較好，深寬比不高情況下，孔徑距/孔徑比對流場影響有限，可以不受孔徑距/孔徑比之限制。在多孔陣列特性上，鍍槽陰極板轉速過高並無實質幫助，配合尺寸規格不同，以低轉速進行製程，不僅節省成本，且可增進產品品質，並可作為多種用途陣列模仁製程重要之參考依據。

關鍵詞：陣列模仁，深寬比，微電鑄，流場分佈

I . INTRODUCTION

Advances in electronic, optoelectronic, energy and biomedical chip products are moving toward small, light and short products in which the microstructure of many important components must be manufactured on a micrometer scale. The traditional process for a micro-hole array structure applied in a bionic chip, micro fluidics sensor, optical communication system or micro fuel cell plate includes refined mechanics micro machining (e.g., μ -EDM and micro-turning) or silicon bulk micro machining. A rough degree for such manufactured products is poor and the process wastes considerable time. Material selection is generally limited and mass-production is not easy. By following the rapid development of micro-electro-mechanical system (MEMS) [1-3] product technology, manufacturing based on LIGA-like can produce a high aspect ratio and high degree of precision of micro mold inserts.

The standard LIGA production procedure uses synchrotron radiation X illuminant with a wavelength of 0.2-0.6nm as the source for micro-lithography of microstructures. By using the micro-electroforming procedure, electroforming products or mold inserts can be manufactured. Because synchrotron radiation X illuminant is not easily obtained and the associated equipment is expensive, using UV light [4-6], an excimer laser [7] or the deep etching [8] process as the LIGA-like of a substitute illuminant have become mainstream. The LIGA-like process can manufacture microstructure with a high degree of precision and high aspect ratio such that micro-electroforming is the best mold insert technology for producing metal structures. For deep and narrow holes, the first task in the micro-electroforming process is to make a plating solution flow and circulates smoothly that replaces the electroforming solution. Additionally, while electroforming nickel, the side reaction of the hydrogen reducing furnace is accompanied by. If the removal rate of hydrogen-bubbles is smaller than the growth rate of the electroforming layer, hydrogen-bubbles will be packed inside the layer and caused defects. Therefore, one must control the flow field of an electroforming solution in deep holes and the hydrogen elimination rate, and the distribution of shearing stress

on the bottom layer of a solution to grow a layer uniformly and smoothly.

Many scholars [9-12] have recently used theoretical analysis or an experimental method to discuss the influence and overcome surface tension created by surfactant with different components or characters to the bubbles and fluid interface. These studies of electroforming generally change operational parameters, such as current density, surfactant, electrode kinetics, plating solution formula, and the electrochemistry angle. These studies have seldom observed the flow field of an inner electroforming solution with the angle of computational fluid dynamics. In fact, based on the fast development of micro-electro-mechanical system, a microstructure with a small aperture and large aspect ratio is generally widely. To finish electroforming a micro-structure when not using traditional wetting agent and leveling agent renewing the plating solution in a deep hole effectively and supplementing the metal ion density to continue reduction must depend on an understanding flow field in the deep hole and mass transfer effects. Kondo [13-16] used the concept of mass transfer in researching micro-electroforming flow field and discussed the relationship between the effects of mass transfer convection and various aspect ratios. It uses practical electroforming to verify and demonstrate that the mass transfer for a hole $\leq 100\mu\text{m}$ is based mainly on the diffusion effect. For a hole $\geq 200\mu\text{m}$, it is based on the convection effect. However, these studies did not analyze the flow field of electro plating solutions and shearing stress of the electroforming mold shape effect in different apertures and aspect ratios. This study uses (CFD-RC) software to simulate the inner micro-electroforming flow field for flow field analysis, and qualitative analysis of the distribution of shearing stress. It is utilized to understand the reaction mechanism that changes plating solution flow field shape, the distribution of shearing stress on nickel ions deposited in a hole array and the influence of uniformity in thickness of the nickel plating layer film. To understand the results obtained by numerical simulation, this study uses ICP-RIE deep etching technology to produce hole arrays with different aspect ratios (depth / (width = aperture)), and electroforms Nickel to make a mold insert to verify the numerical simulation results.

II. NUMERICAL SIMULATION THEORIES AND EXPERIMENTAL METHODS

2.1 Basic Assumption

This study uses an electroforming tank with a rotating cathode below and anode plate above as the basic model (see Fig. 1). With this tank, the micro-hole array mold insert with holes sized $50\mu\text{m}$, $100\mu\text{m}$ and $200\mu\text{m}$ in diameter, models with different aspect ratios can be established. They can be used to discuss the effects of different aperture flow field distributions for a single hole and multiple-hole (e.g., 24 holes) on different cathode rotational speeds. Simulation aspect ratios are 0.5, 1, and 2; the entry flow speeds of the plating solution are 0.01m/s , 0.5m/s and 1m/s . The flow velocity over an open cavity in these models is assumed uniform along the Z-axis. Additionally, the dimension of the Z direction is assumed significantly larger than those in the X and Y directions. Consequently, these models can be approximated in a two-dimension simulation. The primary goal of this study is to determine the optimal operating conditions and parameters with based on experimental results. Thus, this study uses a two-dimension flow field for simulation. The same simulation conditions have been used in other studies¹⁴⁻¹⁷. To retain the simplicity of the basic micro electroform model and reduce the effects of other factors, we assume the following basic conditions. (1) The flow field solution is a steady state, laminar flow, incompressible flow and non-turbulent flow. (2) Heat transfer is not considered. The internal temperature remains constant. It is an isothermal flow, and no energy diversion exists during heat transfer. (3) The physical condition of the diffusion coefficient, Γ and density of the plating solution are fixed.

The simulation fluid is nickel-plating solution. The physical parameters of this solution are as follows. Temperature: $T=327^\circ\text{K}$ (generally $317^\circ\text{K}\sim 347^\circ\text{K}$ during electroforming). Density: $\rho=1100\text{kg/m}^3$. Viscosity Factor: $\nu=2\times 10^{-3}\text{kg/sm}$. Diffusion coefficient: $\Gamma=1\times 10^{-10}\text{m}^2/\text{sec}$. Consistency: $C=5\%$ (percentage).

The fixed distance R from the cathode plate rotational center to holes is 1 mm. The cathode

is rotated to face downward, while the anode faces upward in the standard model. Mesh building of CFD-RC is applied to generate the geometrical model. Figure 2 presents the boundary conditions and geometrical model. The hole on the left side is entry flow speed. The hole on the right side is an outlet. The hole and photo-resist on the upper is the pressure surface (i.e., the pressure gradient is zero). The photo-resist and cathode surface are the walls. The case simulation was performed about 2000 times by a computer. The value of convergence error is $1.0\text{E}-8$ during each simulation to fit the requirement.

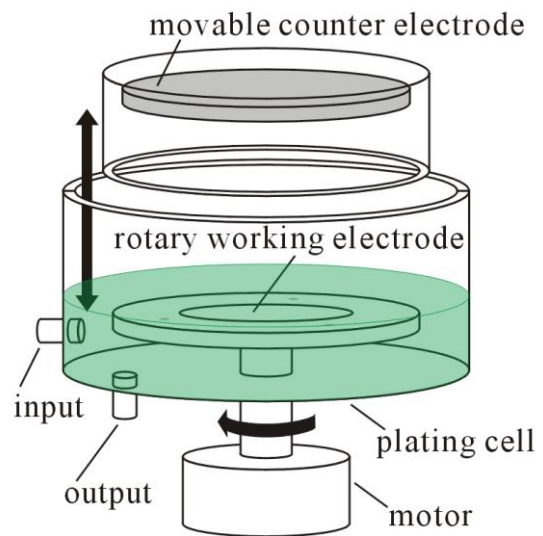


Fig. 1. The diagram of micro-electroforming plating tank.

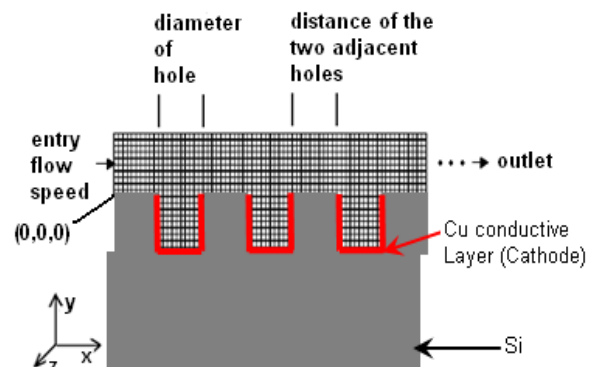


Fig. 2. Geometrical diagram of micro-electroforming hole.

2.2 Governing Equation

This study obtains numerical results calcu-

lated by a CFD package, and evaluates the fluid speed and the distribution of shearing stress iteratively. To simulate precisely the flow field distribution of aspect ratio micro electroforms hole, the Finite Volume Method is used as the numerical method and mathematical mode. Micro electroforming is an electrochemical reaction, which is the same as electroplating. Metal ions or compound metal ions are deposited on the surface of a work piece. The electrochemical reaction in the deposition process has governing equations for inner flow field analysis of laminar flow motion. Such an equation comprises a group composed by mass, momentum and energy of non-isentropic flows following the conservation principle of the Reynolds Transport Theorem, and is called the Navier Stokes equation. By calculating the variance (S) in statistics, one can determine the departure range between the number created by calculating for each data group and the mean value of all data groups. As variance decreases, the degree of the change for that data group decreases. That is, the change to, and tendency of, the data distribution curve will be gentle and mild. The size of shearing stress variance can be used as a basis to determine the uniformity for shearing stress distribution in the hole bottom. As variance in decreases, uniformity of increases. Conversely, as variance increases, uniformity decreases. The formula is defined and listed below.

$$S^2 = \frac{1}{n-1} \sum (x - \bar{X})^2 \quad (1)$$

2.3 Electroforming Experience

This study applied the dry etching technique in the inductively coupled plasma-reactive ion etching (ICP-RIE) method to produce a columniform Si template. Lithography was applied first to define the pattern, and was then followed by ICP-RIE etching using silicon dioxide (SiO₂) as a resist. The 200 nm Cu films (conductive layer of electroforming) were deposited at a power of 500W in a sputtering system using a sputtering pressure of 6.4mTorr after base pressure was evacuated to below 5x10⁻⁷ Torr.

A rotary cathode in a cylindrical vertical electroforming tank was designed as shown in

Fig. 1. The power supply was controlled using a potentiostat/golvanostat (EG&G 263) and Head Start software (provided by EG&G). Current output and current density were controlled via program interface. Table 1 presents the nickel-plating solutions and operating conditions. A Cu-sputtered conduction wafer was first immersed in 5% sulfuric acid to activate the wafer. The wafer was then cleaned in deionized water and electroforming conditions were set. Electroforming conditions include cathode rate of rotation, current density, pH, temperature, additive and concentration. The micro-electroforming process was then performed. When the electroforming process is finished, the micro-hole array mold insert is released by KOH (concentrations 25 weight %. at 72 °C), washed with de-ionized water and dried in an oven. The nickel micro-hole array is then being observed by SEM.

Table 1. Composition of Ni electroforming solution and conditions of Electroforming

Description	Concentration
Nickel sulfate	480 ml/L
Boric acid	40 g/L
Saccharin	1 g/L
Sodium lauryl sulfate	2 ml/L
Current density	1–5 ASD
pH	3.8–4.2
Temperature	50°C

III. RESULTS AND DISCUSSION

This study simulates changes to micro-hole array mold inserts of various sizes to generate micro-electroforming single holes with different apertures, and changes to aspect ratios to simulate shearing stress and speed field under different cathode rotational speeds. Finally, this study simulates the comparative relation produced by changes in holes number for each hole in multi-hole array (24 holes are used as an example).

3.1 Entry Flow Speed Effect

Figure 3 shows when the aperture is 50μm and 100μm, the inner rate of hole isograms have an aspect ratio of 1. The entry flow speed closest to the cathode electroforming area moves

through plating solution and flows out of the outlet. Because the velocity is influenced by the protruding of flow channel while nearing the hole, shearing stress gathers at the hole edge. Thus, on both sides of the hole, shearing stress will be large. As the width of the hole decreases, shearing stress increases. This is because the solution is influenced by hole width and vortex phenomena increases the velocity gradient. When the hole width of an object for plating is small ($50\mu\text{m}$), the shearing stress value will be great. The width of the hole is wider ($100\mu\text{m}$), the shearing stress value will be small. Thus, the convection effect is greater than diffusion effect in mass transfer for a wide hole. Additionally, the diffusion effect is greater than the convection effect in mass transfer for narrow hole. As the size of the hole decreases, the size of the vortex increases. Furthermore, when the width of the hole is $50\mu\text{m}$ (Fig. 3a) a single vortex appears. For a hole with a width of $100\mu\text{m}$ (Fig. 3b) a dual-vortex appears. Such phenomena are the same as numerical results acquired by Kondo¹⁴⁾ et al. For the change to shearing stress variance with an aperture of $50\mu\text{m}$ (Fig. 4a), the shearing stress field is not influenced significantly by entry flow speed. Shearing stress variance for different entry flow speeds is influenced markedly by cathode rotational speed. The change in shearing stress variance with an aperture of $50\mu\text{m}$ follows the change in cathode rotational speed of 0~500 rpm. The variance changes of inlet velocity for 0.01 m/s, 0.05 m/s and 1 m/s are 0.004~711, 13~672 and 55~636 respectively. When the cathode rotational speed is ≤ 100 rpm, the change degree is small. That is, the bottom shear stress for cathode rotational speed in the $50\mu\text{m}$ aperture is uniform. As rotation rate increases, the influence of centrifugal force increases. The upward flush speed increases, the side shearing stress of the hole will also be influenced and non-mixed action is created. In the micro-electroforming process, both side-structure of the hole should be noticed. The change to shearing stress variance with an aperture of $100\mu\text{m}$ (Fig. 4b) will be ≤ 35 at different entry flow speeds. With an increase in rotation rate, variation does not change significantly. The uniformity of shearing stress field is good. Comparing the changes in shearing stress field for apertures of $50\mu\text{m}$ and $100\mu\text{m}$ (Fig. 4), shearing stress variance for an aperture of $50\mu\text{m}$

is influenced by the cathode rotational speed markedly and less in entry flow speed. The shearing stress variance for an aperture of $100\mu\text{m}$, with an aspect ratio of 1 is 0~35. Indicating the different inlet velocities and cathode rotational speeds do not have markedly influence the shearing stress field. Thus, the uniformity of shearing stress field is good.

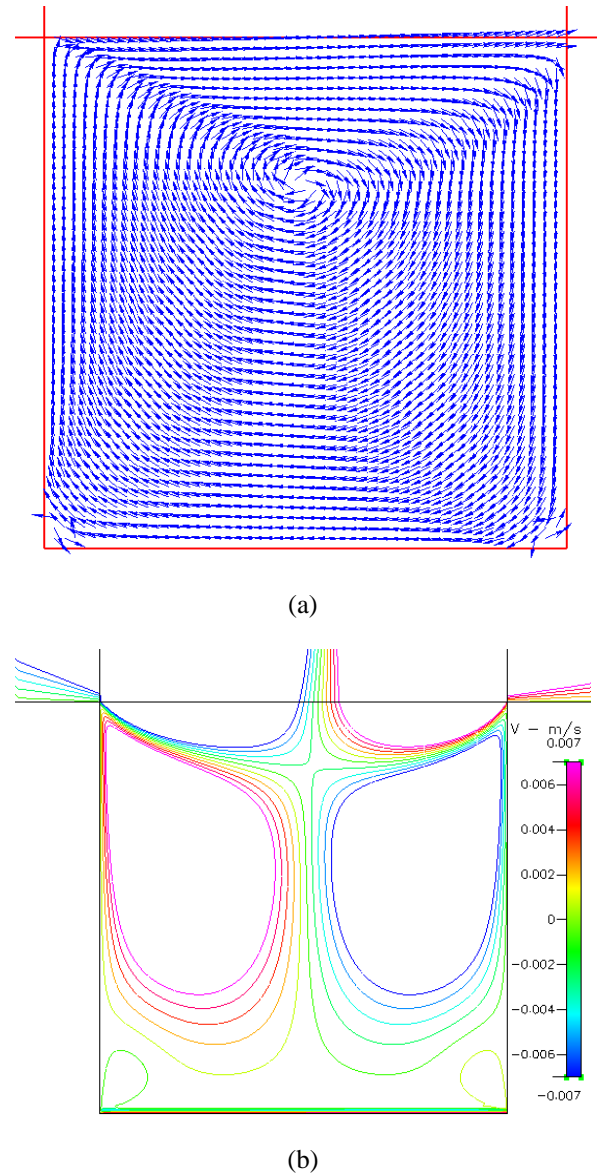
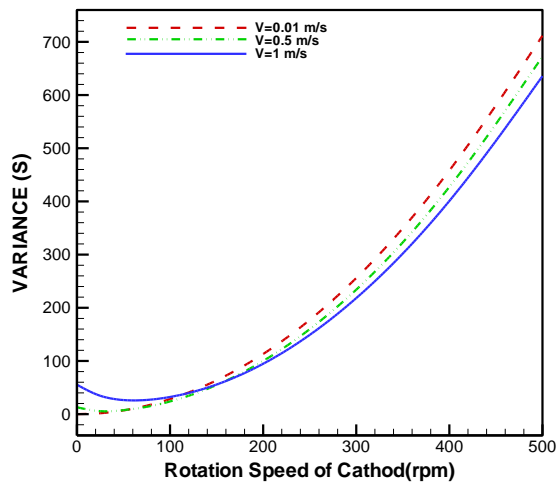
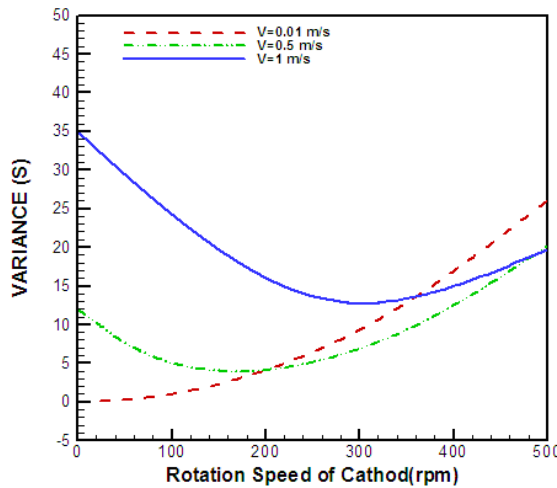


Fig. 3. The speed of nickel plating solution is 1 m/s with aspect ratio 1 and the cathode rotational speed is 0rpm: (a) the inner flow field speed vector for the diameter of the hole with $50\mu\text{m}$, (b) the distribution of flow speeds for the diameter of the hole with $100\mu\text{m}$.



(a)



(b)

Fig.4. The shearing stress variance and the cathode rotational speed for the diameters of the holes in: (a) 50 μm , (b) 100 μm , when the entry flow speed of nickel plating solution is different and the aspect ratio is 1.

The variance changes of shearing stress for all single holes with different diameters. Figure 5 presents analytical results for diameters of 50 μm , 100 μm and 200 μm . When the entry flow speed of the nickel-plating solution is 0.01 m/s and the aspect ratio is 1, shearing stress variance increased following the increase in cathode rotational speed. Indicating the uniformity of shearing stress field degrades at high rotational speeds. As hole diameter decreases, the variance of shearing stress increases. Meaning the uniformity of shearing stress field is also worse. In addition, this study observed the diameter of a hole 50 μm with an aspect ratio of 1. When

cathode rotational speed reaches 50 rpm and 500 rpm (Fig. 6), the following result is obtained. As aperture size decreases, shearing stress increases.

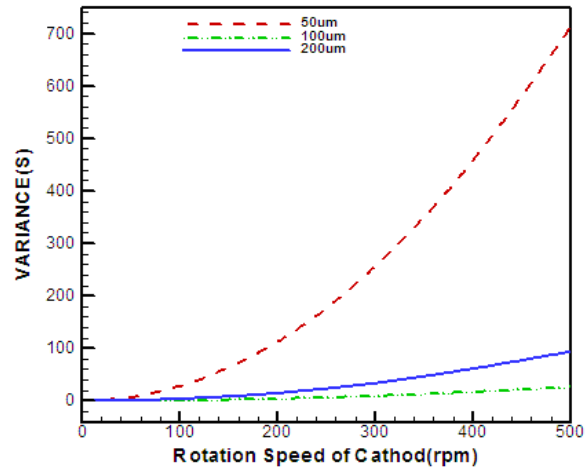


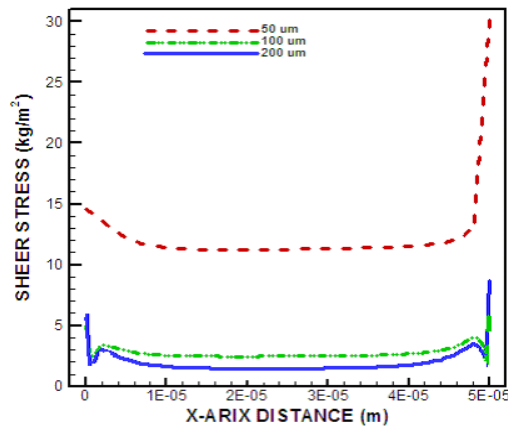
Fig. 5. The shearing stress variance and the cathode rotational speed with different diameters of micro-hole, with aspect ratio in 1 and with the entry flow speed of nickel plating solution in 0.01 m/s.

Additionally as cathode rotational speed increases, shearing stress increases. A large rotation rate causes the variance of side shearing stress increase. From the formula $\tau = \mu du/dy$, the value of shearing stress can be acquired. As the velocity gradient decreases, shearing stress decreases. Conversely, as the velocity gradient increases, shearing stress increases. Due to a small aspect ratio for a hole and near the hole middle shearing stress in the flow field appears fixed value due to the affect of the linear-change rate. However, near the hole sidewall shearing stress increases and form the situation of “boundary straight” due to bearing the velocity from the bottom and velocity from the hole side wall. Thus, during micro electroforming, one must consider the side growing structure for a hole with a small diameter.

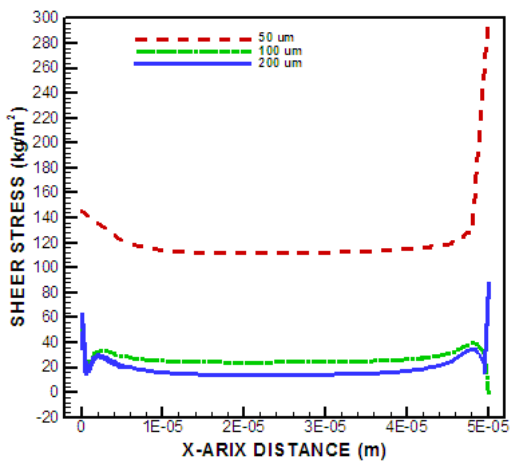
3.2 Effect of Different Aspect Ratios

Observation of micro-holes with different sizes indicates that shearing stress is influenced by aspect ratio and cathode rotational speed. As hole diameter decreases and aspect ratio increases, the variance change to shearing stress increases (Fig. 7) following the increase in

cathode rotational speed. As hole diameter increases, the degree of uniformity for the shearing stress field increases, which is influenced by aspect ratio and the cathode rotational speed. However, the shearing stress field will have great change when influenced by rotation rate in a high aspect ratio. That is, when the aspect ratio is high, the cathode rotational speed affects the degree of uniformity of the shearing stress field. The degree of uniformity for the bottom shearing stress field with a high aspect ratio is poor under fast rotation. When cathode rotational speed increase, the size of the transverse side shearing stress is not uniform and influences the deposit uniformity of plating solution. Thus, as cathode rotational speed increases, the greater the high aspect ratio influenced by side shearing stress field in uniformity of deposit will be.

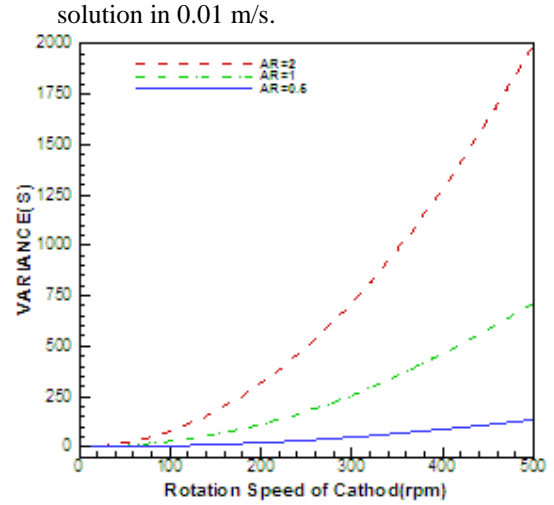


(a)

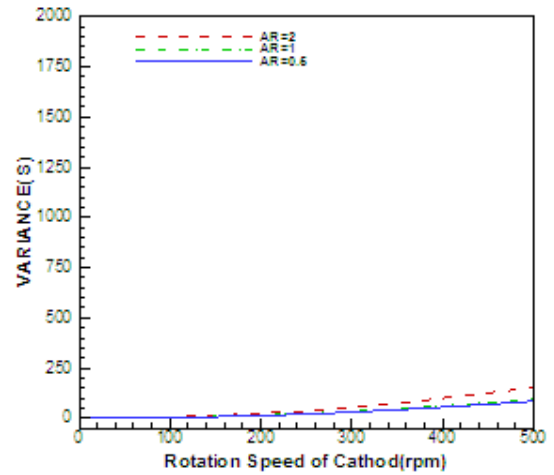


(b)

Fig. 6. The shearing stress distribution for the bottom of cathode with different diameters of micro-hole, with the cathode rotational speed in: (a) 50 rpm, (b) 500 rpm, with aspect ratio in 1, and with the entry flow speed of nickel plating



(a)



(b)

Fig. 7. The variance of shearing stress of different aspect ratio and the cathode rotational speed with the diameters of holes in: (a) 50 μ m, (b) 200 μ m, and the entry flow speed of nickel plating solution in 0.01 m/s.

3.3 Variation Comparison and Analysis for Each Hole in the Multi-Hole Array

A multi-hole array is constructed based on the following conditions: the array has 24-holes; hole diameter is 100 μ m; aspect ratio is 1; and the ratio of hole distance to hole diameter is 1:1. By observing the holes 1, 13 and 24 when entry flow speed is 1 m/s, based on the change breadth in shearing stress variance (Fig. 8) it is enlarged by as rotational rate increases. In the hole, which is far from the rotational center, following the increase in cathode rotational speed, shearing stress variance changes more violently and

markedly. The increase in cathode rotational speed accelerates the exchange rate of plating solution for holes far from the rotational center. The difference between upward flush speed and downward flush speed is great. For holes far from the rotational center, the rate (downward flush speed) of plating solution entering to the hole cannot catch up with the upward flush speed following an increase in cathode rotational speed. Although the exchange rate increased, it cannot reach a balance between upward flush speed and downward flush speed. Following increases in cathode rotational speed, as the distance between holes and the rotational center increases, the unevenness of the shearing stress field increases. For holes in the multi-hole array, as the distance between the hole and rotational center increases following the increase in cathode rotational speed, the unevenness in physical property will be. And the deposit of plating solution will be uneven. Therefore, when the aspect ratio is 1, a cathode rotational speed of 100rpm is best (Fig. 8).

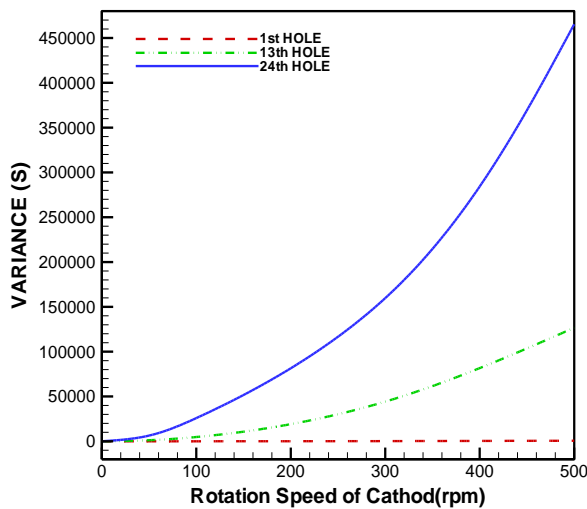
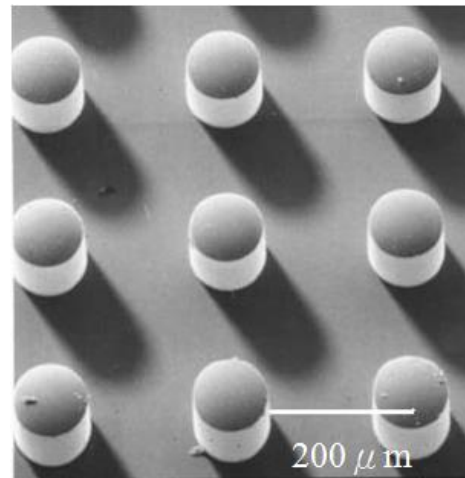


Fig. 8. The bottom shearing stress variance for each hole and the cathode rotational speed with 24 holes array, with the diameter of hole in $100\mu\text{m}$, with the aspect ratio in 1, with the ratio for distance of hole and diameter of hole in 1, and the entry flow speed of nickel plating solution in 1 m/s .

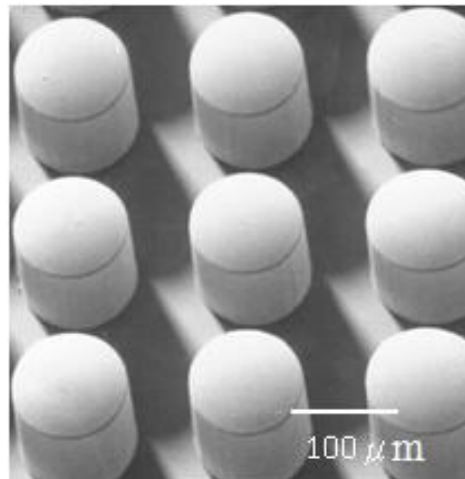
3.4 Experimental Verification of Micro-electroforming

The flow field analysis for a single micro-hole or micro-hole array with different hole

diameters and aspect ratios has been described in detail. The cathode rotational speed for the single microstructure electroforming process of micrometer scale is important parameter that can, depending on parameter value, can create good or bad mold insert electroforming. Based on numerical simulation results for multiple micro-holes (micro-hole array) with a regular arrangement, the aspect ratio ≤ 2 , and the influence of cathode rotational speed on the electroforming mold insert is reduced.



(a)

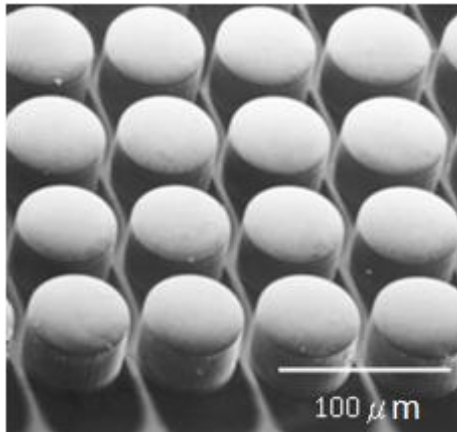


(b)

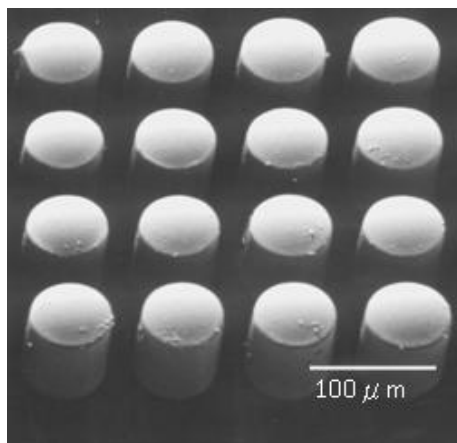
Fig. 9. Micro-hole array mold insert for electroforming nickel with the diameter of the hole in $100\mu\text{m}$, with: (a) aspect ratio is 1, (b) aspect ratio is 2.

In other word, the array mold insert is easily worked, and its reliability can be improved significantly. We believe such data are helpful when designing and manufacturing micro-hole array with various utilities. To understand the

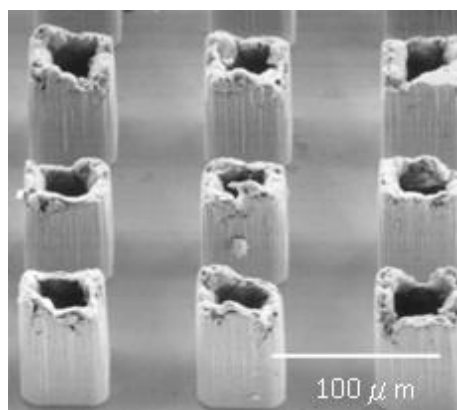
relationship between numerical simulation results and the real electroforming mold insert, this research carried out an electroforming experiment for a hole array with hole diameters ≤ 100 micrometer and with aspect ratios ≤ 2 .



(a)



(b)



(c)

Fig. 10. Micro-hole array mold insert for electroforming nickel with the diameter of the hole in $50\mu\text{m}$, with: (a) aspect ratio is 1, (b) aspect ratio is 2, (c) aspect ratio is 4.

Figure 9 presents a nickel metal micromold produced using an Si template with a holes diameter $=100\mu\text{m}$, aspect ratios of 1 and 2 and a cathode rotational speed of 100 rpm. The external structure is complete and the mold is effectively duplicated. Figure 10 presents nickel micro-mold produced using an Si template with holes $=50\mu\text{m}$ in diameter and aspect ratios of 1, 2 and 4 at a cathode rotational speed of 100 rpm. From Fig.10(c) that it will not acquire a whole nickel mold figure with the same electrochemistry deposit condition when the aspect ratio is greater than 2. Therefore the exchange rate of plating solution for the holes with same diameter and smaller aspect ratio value will be better. Based on electroforming results electroforming molds with holes arrays with low aspect ratios (aspect ratio ≤ 2) can be fabricated at low cathode rotational speeds. Therefore, numerical simulation of the flow field is useful for determining the suitable rotational speeds for stimulating various aspect ratios of the electroforming molds process.

IV. CONCLUSIONS

Numerical simulation results show that when a hole with a diameter between $50\mu\text{m}$ and $200\mu\text{m}$ and aspect rate of ≤ 2 , the effect of cathode rotational speed on the electroforming mold insert can be reduced. Thus, one can easily obtain the best electroforming mold insert. A small entry flow speed for the plating solution causes the efficiency of the exchange rate for the plating solution will be bad. The entry flow speed of the plating solution should be accelerated to increase the exchange rate of the plating solution. A high cathode rotational speed is not necessary. Thus, a large shearing stress variance and an uneven stress field can be avoided and the deposit uniformity is affected.

The exchange rate efficiency of the plating solution with a low aspect ratio is superior to that at a high aspect ratio. For the hole with a small diameter and a high aspect ratio, the downward flush speed increases when cathode rotational speed accelerates. However, exchange plating solution from the hole is difficult. The old plating solution will be increased and is harmful to the exchange of plating solution. Thus, the aspect ratio must be reduced to generate a good exchange of plating solution. For mi-

cro-hole array mold inserts with different dimensions, the shearing stress field will be uneven following an increase in cathode rotational speed. Therefore, to enhance exchange rate efficiency of the plating solution, uneven stress, which is caused by the increase in cathode rotational speed and affects the growth uniformity, must be considered. In this study, a high cathode rotational speed was not suitable when the aspect ratio was low. The cathode rotational speed should be set at 100rpm-300rpm according to the different holes diameters.

For the multi-hole array, based on the exchange rate for the plating solution, the variance of shearing stress field for the hole, that is far from the rotational center is influenced by cathode rotational speed. A high cathode rotational speed causes unevenness in the deposition rate. To avoid this unevenness in shearing stress for holes far from the rotational center, the cathode rotational speed and aspect ratio should not be high. Based on practical electroforming results, when a single hole with a diameter ≥ 50 micrometer and aspect ratio ≤ 2 , the influence of the cathode rotational speed on the electroforming mold insert can be reduced to the lowest; this is beneficial to manufacturing the best electroforming mold insert.

REFERENCES

- [1] Chin, T. S., "Permanent Magnet Films for Applications in Microelectromechanical Systems," *Journal of Magnetism and Magnetic*, Vol. 209, pp. 75-79, 2000.
- [2] Chan, Y. C., Miao, J. M., Wang, S. S., and Chuang, T. H., "Simulation Analysis of Electroplating Process for Flip-Chip Solder Bumps," *Journal of Materials Science and Engineering*, Vol. 34, No. 1, pp. 8-16, 2002.
- [3] Spearing, S. M., "Materials Issues in Microelectromechanical Systems (MEMS)," *Acta mater*, Vol. 48, pp. 179-196, 2000.
- [4] Wenmin, Q., Christian, W., and Gerald, G., "Fabrication of a 3D differential-capacitive acceleration sensor by UV-LIGA," *Sensors and Actuators* 77, pp.14-20, 1999.
- [5] Williams, J. D., Yang, R., and Wang, W., "Numerical simulation and test of a UV-LIGA-fabricated electromagnetic micro-relay for power applications," *Sensors & Actuators: A. Physical*, Vol. 120, pp. 154-162, 2005.
- [6] Li, B. and Chen, Q., "Solid micromechanical valves fabricated with in situ UV-LIGA assembled nickel," *Sensors & Actuators: A. Physical*, Vol. 126, pp. 187-193, 2006.
- [7] Choi, K. H., Meijer, J., Masuzawa, T., and Kima, D. H., "Excimer laser micromachining for 3D microstructure," *Journal of Materials Processing Technology* Vol. 149 pp. 561-566, 2004.
- [8] Michael, P. L., "Arbitrarily profiled 3D polymer MEMS through Si micro-moulding and bulk micromachining" *Microelectronic Engineering* Vol. 83, pp.1257-1260, 2006.
- [9] Daniel, R. C. and Berg, J. C., "A simplified method for predicting the dynamic surface tension of concentrated surfactant solutions," *Journal of Colloid and Interface Science*, Vol. 260, No. 1, pp. 244-249, 2003.
- [10] Loubier, K. and Hebrard, G., "Influence of liquid surface tension (surfactants) on bubble formation at rigid and flexible orifices," *Chemical Engineering and Processing*, Vol. 43, pp. 1361-1369, 2004.
- [11] Miller, R., Fainerman, V. B., Leser, M. E., and Michel, M., "Surface tension of mixed non-ionic surfactant/protein solutions: comparison of a simple theoretical model with experiments," *Colloids and Surfaces A: Physicochemical and Engineering Aspects*, Vol. 233, pp. 39-42, 2004.
- [12] Landolt, D., "Electrodeposition Science and Technology in the Last Quarter of the Twentieth Century," *Journal of the Electrochemical Society*, Vol. 149 No. 3 S9-S20, 2002.
- [13] Kondo, K., Fukui, K., Uno, K., and Shinohara, K., "Shape Evolution of Electrodeposited Copper Bumps," *J. Electrochem. Soc.*, Vol. 143, No. 6, pp. 1880-1886, 1996.
- [14] Kondo, K. and Fukui, K., "Shape Evolution of Electrodeposited Bumps with Deep Cavity," *J. Electrochem. Soc.*, Vol. 145, pp. 3007-3010, 1998.
- [15] Kondo, K. and Fukui, K., "The Current Evolution of Electro Deposition Copper Bumps with Photoresist Angle," *J. Electrochem. Soc.*, Vol. 145, pp. 840-843, 1998.
- [16] Hayashi, K., Fukui, K., Tanaka, Z., and Kondo, K., "Shap Evolution of Electrodeposited Bumps into Deep Cavity," *J. Electrochem.Soc.*, Vol.148,C145-C148, 2000.